

PAPER • OPEN ACCESS

## Effect of $\text{ZnFe}_2\text{O}_4$ Filler Loading on the Morphology and Mechanical Properties of Epoxidised Natural Rubber 25 (ENR 25)

To cite this article: Suziey Syamimi Sukri *et al* 2020 *IOP Conf. Ser.: Earth Environ. Sci.* **596** 012043

View the [article online](#) for updates and enhancements.



EEG/ECOG AMPLIFIERS  
& ELECTRODES  
ELECTRICAL/CORTICAL  
STIMULATORS  
REAL-TIME PROCESSING

**g.tec**  
gtec.at/shop  
SHOP NOW

# Effect of ZnFe<sub>2</sub>O<sub>4</sub> Filler Loading on the Morphology and Mechanical Properties of Epoxidised Natural Rubber 25 (ENR 25)

Suziey Syamimi Sukri<sup>1</sup>, Syifa' Muhamad Sharifuddin<sup>1</sup>, Mohd Shukri Mat Nor<sup>1</sup>, Fathin Asila Mohd Pabli<sup>1,2</sup>, Julie Juliewatty Mohamed<sup>1</sup>, Wannarat Chueangchayaphan<sup>3</sup> and Muhammad Azwadi Sulaiman<sup>1,\*</sup>

<sup>1</sup>Advanced Materials Research Cluster, Faculty of Bioengineering and Technology, Universiti Malaysia Kelantan, 17600 Jeli, Kelantan, Malaysia.

<sup>2</sup>Politeknik Mukah, 96400 Mukah, Sarawak, Malaysia.

<sup>3</sup>Faculty of Science and Industrial Technology, Prince Songkla University, Surat Thani Campus, Surat Thani 84000, Thailand.

Email: azwadi@umk.edu.my

**Abstract.** In this study, the effect of ZnFe<sub>2</sub>O<sub>4</sub> loading on the morphology and mechanical properties of epoxidised natural rubber 25 (ENR 25) was intensively investigated. The composite densities were measured using a density meter. The morphological analyses were characterised by scanning electron microscopy. The mechanical properties, including hardness, stress-strain behaviour, tensile strength, elongation at break, and tensile modulus were also investigated. The present rubber ferrite composite showed a particulate dispersion of ZnFe<sub>2</sub>O<sub>3</sub> on its morphological surface. The composite also presented characteristic of high density (1.592 g/cm<sup>3</sup>), hardness (44.63 Shore A at 120 phr), high tensile strength (14.09 MPa at 80 phr), high elongation at break (648.79 % at 120 phr), and high tensile modulus (100% modulus: 1.05% at 120 phr, 300% modulus: 1.93 MPa at 80 phr) compared to the ENR 25 without filler which is 1.006 g/cm<sup>3</sup>, 28.13 Shore A, 8.49 MPa, 615.18%, 0.65 (100% modulus) and 1.38 (300% modulus) respectively.

## 1. Introduction

Among the electroceramic materials, ferrite remains one of the best because it offers a wide range of the spectrum, inexpensive and stable [1]. Mixed ferrites like zinc ferrites (ZnFe<sub>2</sub>O<sub>4</sub>) are found to have extraordinary thermal, electrical, mechanical and magnetic properties [2]. However, the brittle nature of ferrite has limited its use in an application such as in tunable and bendable device. The solution to the shortfall, flexible materials like rubber can be used to mix with the ferrite. Unification of ferrites in an elastomer matrix produces rubber ferrite composites. The matrix properties of the rubber ferrite composites can be modified to tailor their mechanical properties. Soloman et al. [3] had claimed that the mechanical properties are improved, and the dielectric behaviour of the matrix is modified when ferrite fillers were incorporated into an elastomer. The advantages of the composites over their ceramic counterparts include low cost, capability of high production rates, resistance to corrosion, low weight,



and ease of machining [4]. The mechanical properties of the composites depend much on ceramic fillers, the surface area of the filler, matrix properties, and interfacial condition between the components [5]. In this present work, ENR 25 was used as a polymeric matrix to prepare the composites with  $\text{ZnFe}_2\text{O}_4$  as the filler. The influence of  $\text{ZnFe}_2\text{O}_4$  loadings on the mechanical properties of the  $\text{ZnFe}_2\text{O}_4$ / ENR 25 composites was also examined.

## 2. Experimental

### 2.1. Materials and Mixing Method

The raw materials were mixed in a container containing zirconia ball milling for 24 hours at F15.0 speed consistently. The ratio between raw materials and zirconia ball milling is 1:10, and the solvent medium used in the milling process is ethanol. After that, the samples underwent the calcination process at  $1000^\circ\text{C}$  for 12 hours within  $10^\circ\text{C}/\text{min}$  heating rate.  $\text{ZnFe}_2\text{O}_4$  loaded with epoxidised natural rubber (ENR 25) was formulated by mixing the  $\text{ZnFe}_2\text{O}_4$  with the ENR 25, sulphur, zinc oxide, stearic acid, mercaptobenzothiazole (MBT) and butylated hydroxytoluene (BHT).  $\text{ZnFe}_2\text{O}_4$  loadings used in this study were 0, 20, 40, 60, 80, 100 and 120 phr, respectively. The raw material formulations were incorporated in the internal mixer for 12 minutes at  $160^\circ\text{C}$ . The produced compound was compressed and left for 24 hours at room temperature for the mechanical property analyses.

### 2.2. Measurement of Tensile, Hardness and Density Properties

The tensile test was conducted using the Tinius Olsen Tensile Test Machine at room temperature to determine the stress-strain behaviour of the vulcanisates. Thin sheets of the  $\text{ZnFe}_2\text{O}_4$ / ENR 25 composites at loadings of 0, 20, 40, 60, 80, 100 and 120 phr were cut into dumbbell shape samples of ASTM die type C. The grip separation speed was set up at 500 mm/minute and initial gauge length 20 mm following ASTM D412. The stress-strain parameters, including tensile strength, modulus, and elongation at break, were obtained. The hardness of rubber composites was determined using Shore durometer hardness tester, and the unit was expressed in Shore A (ISO 7619-1). The samples were cut into dimensions of 15 cm  $\times$  15 cm before used for testing. The density of the  $\text{ZnFe}_2\text{O}_4$  /ENR 25 composites was determined using the density meter. This equipment does not measure the specific gravity (relative density) directly, which the relative density measurement is based on the water density at  $4^\circ\text{C}$  ( $1\text{ g}/\text{cm}^3$ ). The density of the samples can be measured with the densimeter either in wet or dry portions. The samples were cut subsequently into 1 cm $\times$ 1 cm piece and inserted into the density meter for the measurement purpose.

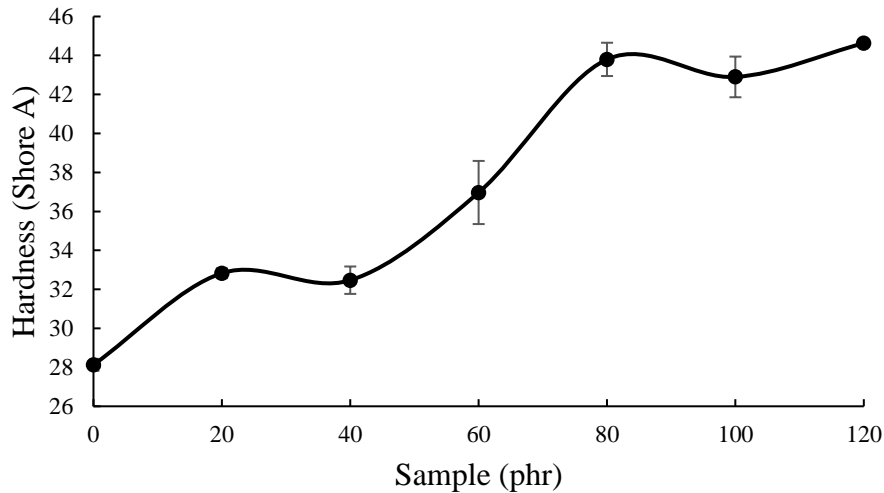
### 2.3. Morphological Analysis

The samples (not coated with any element) were observed using a Scanning Electron Microscope (SEM) JOEL JSMIT 100 under x200 magnification with an accelerating voltage of 3.0 kV and an image width of 100  $\mu\text{m}$ . The samples were cut cross-sections into small pieces and were placed on top of carbon tape on SEM sample mount to allow electron conductivity for better image scanning. SEM morphology analysis was conducted to examine the dispersion of  $\text{ZnFe}_2\text{O}_4$  with ENR 25.

## 3. Results and Discussion

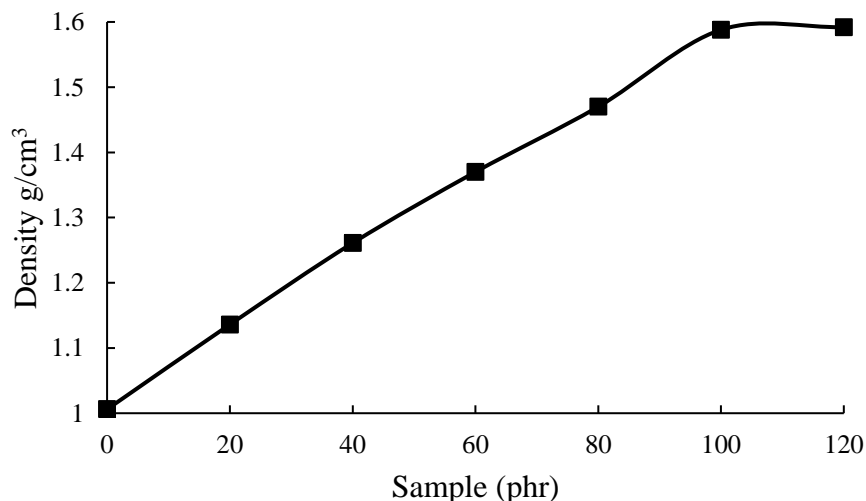
Figure 1 shows the hardness of  $\text{ZnFe}_2\text{O}_4$  loaded ENR 25 with different content of fillers. Generally, the hardness of  $\text{ZnFe}_2\text{O}_4$  /ENR 25 composite increases with the increase of filler loadings, but small depletion in hardness occurred during 40 and 100 phr loadings. From the figure, it can be observed that the hardness of the ENR 25 increases from 28.13 to 32.83 Shore A after adding 20 phr  $\text{ZnFe}_2\text{O}_4$ . However, the hardness of the composite reduces after incorporation of 40 phr  $\text{ZnFe}_2\text{O}_4$  filler given the read of 32.47 Shore A. From 60 to 80 phr loadings, the hardness increases from 36.97 to 43.8 then drops to 42.9 Shore A at 100 phr. The composite exhibits the highest hardness value at 120 phr  $\text{ZnFe}_2\text{O}_4$  loading with 44.63 Shore A. The increasing of  $\text{ZnFe}_2\text{O}_4$  / ENR 25 composite hardness is proportional to

the quantity of  $\text{ZnFe}_2\text{O}_4$ . The hardness of the composite was improved by incorporation of  $\text{ZnFe}_2\text{O}_4$  loading as the rigidity of the composite increase because of the decreasing in the mobility of elastomer macromolecular chains. Besides,  $\text{ZnFe}_2\text{O}_4$  particles can also fill the microscopic cavities at various location in the rubber matrices, which also involved an increase of hardness [6].



**Figure 1.** Hardness of  $\text{ZnFe}_2\text{O}_4$  loaded with ENR 25

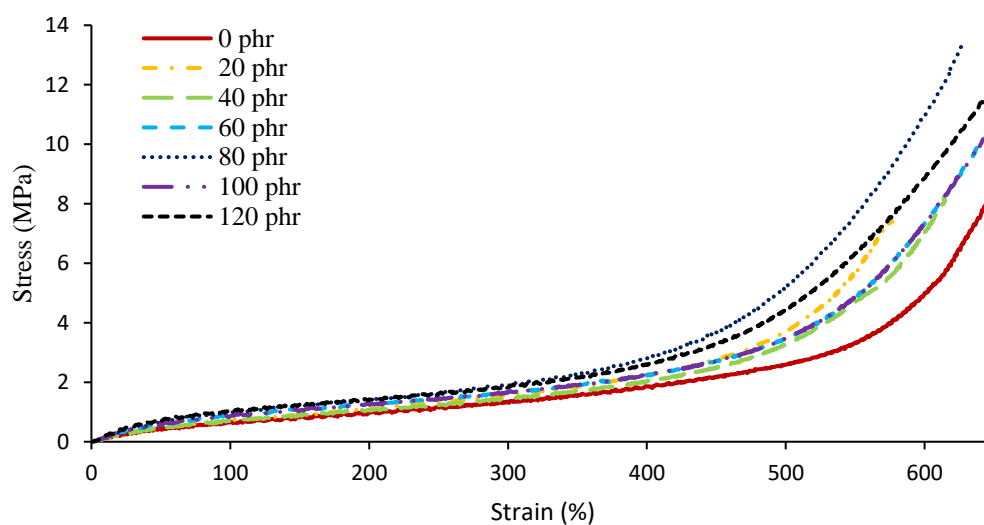
Figure 2 shows the density of ENR 25 loaded with different  $\text{ZnFe}_2\text{O}_4$  filler contents from 0 to 120 phr. The results obtained from density meter show that the density of  $\text{ZnFe}_2\text{O}_4$ / ENR 25 composites increased with increasing of  $\text{ZnFe}_2\text{O}_4$  loadings. The density of the composite is found out to be 1.006, 1.136, 1.261, 1.370, 1.470, 1.588 and 1.592  $\text{g}/\text{cm}^3$  at  $\text{ZnFe}_2\text{O}_4$  loadings of 0, 20, 40, 60, 80, 100 and 120 phr, respectively. The main reason for the increase of the density with the increment of  $\text{ZnFe}_2\text{O}_4$  loadings was owing to a dense material obtained from the  $\text{ZnFe}_2\text{O}_4$  filler. It has been recorded that the density of  $\text{ZnFe}_2\text{O}_4$  is quite high, with 5.32  $\text{g}/\text{cm}^3$  [7].



**Figure 2.** Density of  $\text{ZnFe}_2\text{O}_4$  loaded with ENR 25

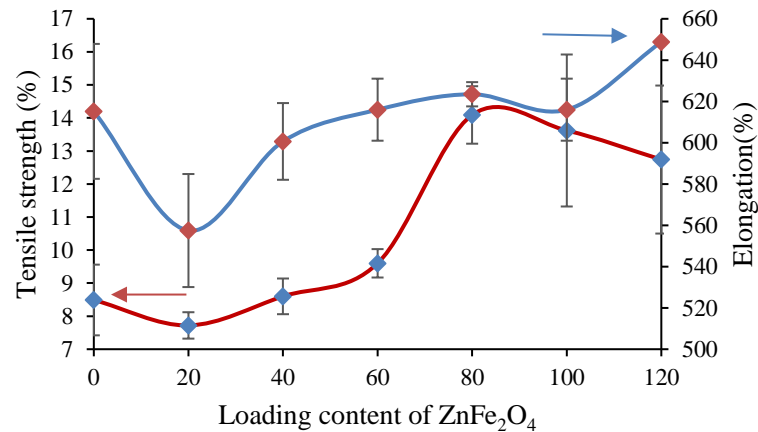
The stress-strain behaviour of the  $\text{ZnFe}_2\text{O}_4$ / ENR 25 composites with different  $\text{ZnFe}_2\text{O}_4$  loadings of 0, 20, 40, 60, 80, 100, and 120 phr is shown in Figure 3. The composites display the increasing of stress-

strain curves, but a drastic increase is observed when strain is higher than 450%. The results occurred due to the high loading of the  $\text{ZnFe}_2\text{O}_4$  that affects the efficiency of a chain in rubber. This trend might be attributable to the rubber self-reinforcing caused by an inclination of the ENR 25 network chains. The phenomenon contributed to the crystallites formation that orient the rubber chains in the direction of the applied stretching force [8]. The filler acts as a nucleating agent to help the rearranging of the molecular chain and fasten the crystal forming under stretched. Higher content of filler in certain limits can increase the reinforcing effects and also promotes greater synergy between ENR 25 and  $\text{ZnFe}_2\text{O}_4$  [9]. It is seen that the 80 phr loading of  $\text{ZnFe}_2\text{O}_4$ / ENR 25 composites presented higher modulus of elasticity than those of the 100 and 120 phr  $\text{ZnFe}_2\text{O}_4$  loadings. This is due to the maximum stress level reached in a strain that caused lower molecular chains mobility, hence increasing the stiffness of the composites.



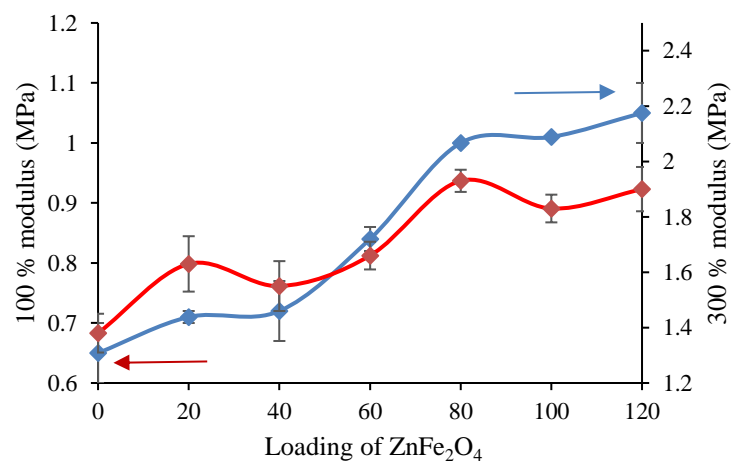
**Figure 3.** Stress-strain of  $\text{ZnFe}_2\text{O}_4$ / ENR 25 composites with different content of  $\text{ZnFe}_2\text{O}_4$  loading

The tensile strength and the elongation at the break of the studied composite against  $\text{ZnFe}_2\text{O}_4$  loadings are illustrated in Figure 4. The tensile strength of  $\text{ZnFe}_2\text{O}_4$ / ENR 25 composite decreases from 0 phr (8.49 MPa) to 20 phr 7.72 MPa, then increased up to 80 phr with the tensile strength of 14.09 MPa. However, samples of 100 to 120 phr show a decreasing of tensile strength with 13.62 to 12.74 MPa, respectively. The result demonstrated that  $\text{ZnFe}_2\text{O}_4$  could play as a reinforcing filler if added below 80 phr. The further increasing of  $\text{ZnFe}_2\text{O}_4$  contents resulted in weak rubber and filler interaction due to the formation of filler agglomeration and dilution effect [10]. The  $\text{ZnFe}_2\text{O}_4$  loadings that appeared on the higher than 80 phr (100 to 120 phr) create the stress point under a stretch condition. This will lead to the constrained motion of the molecular rubber chain, caused decreasing in tensile strength of the composite. This also meant that more addition of  $\text{ZnFe}_2\text{O}_4$  loading ( $> 80$ phr) would not increase the tensile strength of the composite. The irregular trend was discovered for the elongation at break of the  $\text{ZnFe}_2\text{O}_4$ / ENR 25 composites. At the start, the elongation at break decreased from  $\text{ZnFe}_2\text{O}_4$  loadings of 0 phr (615.18%) to 20 phr (557.46%). Then it increased gradually from 20 phr until 80 phr with 600.62% at 40 phr, 615.99% at 60 phr, and 623.46% at 80 phr. However, the elongation at break starts to decrease at 100 phr (615.99%) and increased back again during 120 phr with 648.79%. The reason of the reducing in elongation at break at 20 phr and 40 phr  $\text{ZnFe}_2\text{O}_4$  loadings compared to the 0 phr loading (without filler) might be due to the smaller deformation of  $\text{ZnFe}_2\text{O}_4$  compared to the ENR 25 matrix. As a result, the filler drives the matrix obtaining higher deformation than the produced composite makes it becomes more brittle with the addition of filler.



**Figure 4.** The effect of ZnFe<sub>2</sub>O<sub>4</sub> loading on tensile strength and elongation at the break of ZnFe<sub>2</sub>O<sub>4</sub>/ENR 25 composites.

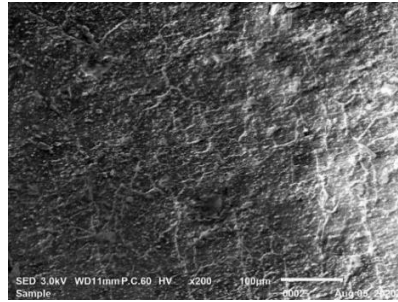
Figure 5 presents the modulus at 100% and 300% strains of ZnFe<sub>2</sub>O<sub>4</sub>/ENR 25 composites. Based on the results obtained by the 100% modulus from the 0 to 120 phr, it can be seen that the trend of the tensile modulus is increasing from 0.65 to 1.05 MPa respectively. This shows that the increase of the loaded ZnFe<sub>2</sub>O<sub>4</sub> affects the modulus at 100% strain might be due to the larger constrain to the molecular motion of the macromolecule [11]. This inclusion caused the bridging of rubber chains between the filler particles improves the modulus at 100% strain [12]. However, the dissimilar trend is presented by the 300% modulus where decreasing of the tensile modulus is shown in the ZnFe<sub>2</sub>O<sub>4</sub>/ENR 25 composites at filler loadings of 40 phr and 100 phr. It is observed that the highest modulus at 300% strain occurred during the loading of 80 phr with 1.93 MPa. This can also be explained by the result of the tensile strength at 80 phr loading. This is believed due to the extensive agglomerated system and low chain interaction after the vulcanisation process [13].



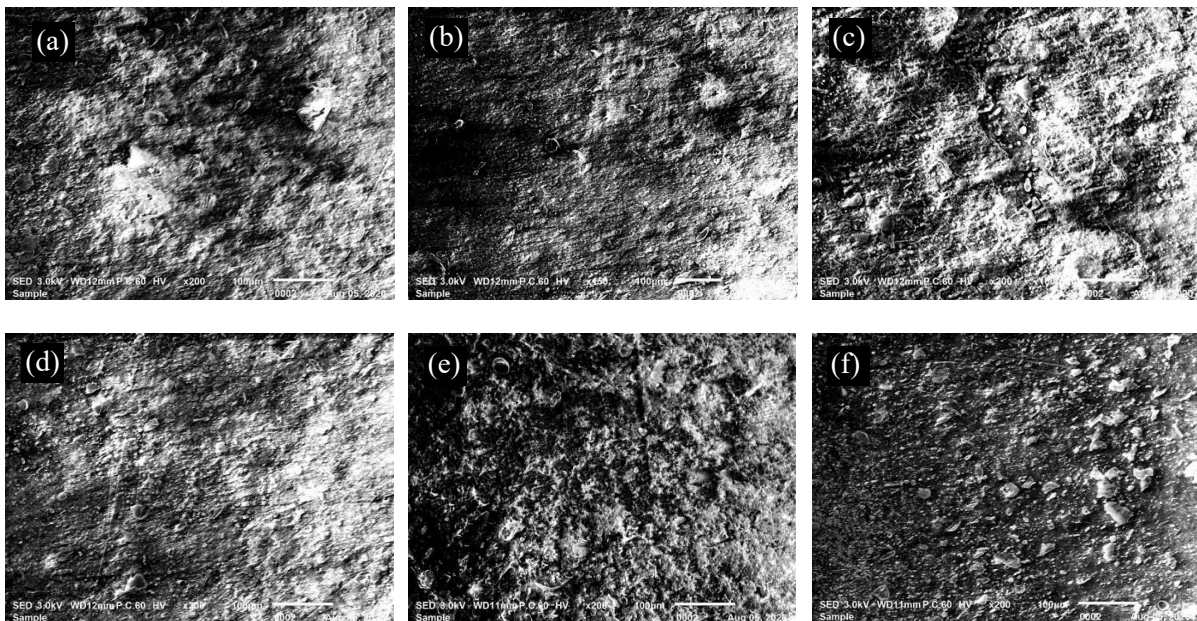
**Figure 5.** The effect of ZnFe<sub>2</sub>O<sub>4</sub> loading on the modulus at 100 and 300% strains of ZnFe<sub>2</sub>O<sub>4</sub>/ENR 25 composites.

Figure 6 and 7 display the SEM observation at 200x magnification of ENR 25 and ZnFe<sub>2</sub>O<sub>4</sub>/ENR 25, respectively. Morphological analysis on the ENR 25 sample without ZnFe<sub>2</sub>O<sub>4</sub> addition shows that the surface structure of the sample has a few microscopic cavities without any embedded particles. Meanwhile, Figure 6 (b) exhibited distinguishable particle agglomeration of ZnFe<sub>2</sub>O<sub>4</sub> in the ENR 25. It

shows the particulate dispersion of the  $\text{ZnFe}_2\text{O}_4$  in the ENR 25 where can be arranged according to loading content of  $\text{ZnFe}_2\text{O}_4$  in the following order: 120 phr > 100 phr > 80 phr > 60 phr > 40 phr > 20 phr. The homogeneous surface dispersions of the  $\text{ZnFe}_2\text{O}_4$ / ENR 25 depend on the loading content of the filler.



**Figure 6.** Morphological Image of ENR 25 (0 phr filler)



**Figure 7.** Morphological Image of  $\text{ZnFe}_2\text{O}_4$ / ENR 25 composites at (a) 20 phr, (b) 40 phr, (c) 60 phr, (d) 80 phr, (e) 100 phr and (f) 120 phr.

#### 4. Conclusion

The results achieved by the study revealed that  $\text{ZnFe}_2\text{O}_4$  incorporated into the ENR 25 matrix influences both the hardness and density of the composite.  $\text{ZnFe}_2\text{O}_4$ / ENR 25 composites were found harder and denser than the pure ENR 25. Generally, the hardness and density of  $\text{ZnFe}_2\text{O}_4$ / ENR 25 composites increase along with the increasing of  $\text{ZnFe}_2\text{O}_4$  loading. SEM at x200 magnification showed that  $\text{ZnFe}_2\text{O}_4$ / ENR 25 composites had increased  $\text{ZnFe}_2\text{O}_4$  agglomeration with an increase in the loading content. The stress-strain behaviour of the  $\text{ZnFe}_2\text{O}_4$ / ENR 25 composites shows a drastic increase above 450% strain while 80 phr loading presented a higher slope of the stress-strain curve than 100 and 120 phr  $\text{ZnFe}_2\text{O}_4$  loadings. Moreover,  $\text{ZnFe}_2\text{O}_4$ / ENR 25 composites have generally improved the results of the tensile strength and elongation at break. Based on the tensile strength results, 80 phr of  $\text{ZnFe}_2\text{O}_4$  loading is the most superior, and its power was decreased with further loading. It is observed that the 80 phr loading displays the highest modulus at 300% strain. This indicates that the produced composites at

80 phr ZnFe<sub>2</sub>O<sub>4</sub> loading are the most optimum condition to balance the mechanical properties due to the efficiency of the network in rubber composites.

## 5. Acknowledgment

This research work was financially supported by the Ministry of Higher Education (MOHE) through the Fundamental Research Grant Schemes (FRGSs): R/FRGS/A1300/0880A/003/2018/00557 (FRGS/1/2018/TK05/UMK/02/5) and R/FRGS/A08.00/00880A/002/2014/00174 (FRGS/1/2014/SG06/UMK/02/1). This special appreciation also for the technical research and supports towards the students' welfare during the Students Mobility Programme between Faculty of Bioengineering and Technology, University Malaysia Kelantan and Faculty of Science and Industrial Technology, Prince of Songkla University, Surat Thani Campus, Thailand.

## References

- [1] Anantharaman M R, Sindhu S, Jagatheesan S, Malini K A, and Kurian P 1999 Dielectric properties of rubber ferrite composites containing mixed ferrites *J. Phys. D. Appl. Phys.* **32** (15) 1801, 1999.
- [2] Kmita A, Pribulova A, Holtzer M, Futas P, and Rocznik A 2016 Use of specific properties of zinc ferrite in innovative technologies *Arch. Metall. Mater.* **61** (4) 2141–2146.
- [3] Solomon M A, Kurian P, Anantharaman M R, and Joy P A 2004 Evaluation of the magnetic and mechanical properties of rubber ferrite composites containing strontium ferrite *Polym. Plast. Technol. Eng.* **43** (4) 1013–1028.
- [4] Makled M H, Matsui T, Tsuda H, Mabuchi H, El-Mansy M K, and Morii K 2005 Magnetic and dynamic mechanical properties of barium ferrite-natural rubber composites *J. Mater. Process. Technol.* **160** (2) 229–233.
- [5] Xiao J and Otaigbe J U 2000 Polymer bonded magnets. II. Effect of liquid crystal polymer and surface modification on magneto-mechanical properties *Polym. Compos.* **21** (2) 332–342.
- [6] Kruželák J, Dosoudil R, Sýkora R, and Hudec I 2014 Rubber composites with incorporated magnetic filler *Polimery/Polymers* **59** (11–12) 819–824.
- [7] Villars P and Cenzual K Eds. ZnFe<sub>2</sub>O<sub>4</sub> Crystal Structure: Datasheet from 'PAULING FILE Multinaries Edition - 2012 in SpringerMaterials ([https://materials.springer.com/isp/crystallographic/docs/sd\\_0547901](https://materials.springer.com/isp/crystallographic/docs/sd_0547901)). Springer-Verlag Berlin Heidelberg & Material Phases Data System (MPDS) Switzerland & National Institute for Materials Science (NIMS), Japan.
- [8] Sulaiman M A, Panwiriyyarat W, Jie B L C, Masri M N, and Yusuff M 2016 Mechanical and Electrical Properties of TiO<sub>2</sub> Loaded Vulcanized Natural Rubber *Int. J. Electroact. Mater.* **4** 39–43.
- [9] Zhang F, Liao L, Yongzhou W, Yueqiong W, Huang H, Puwang L I, Zheng P, and Rizhong Z 2016 Reinforcement of natural rubber latex with silica modified by cerium oxide: Preparation and properties *J. Rare Earths* **3** (2) 221–226.
- [10] Ismail H, Sam S T, Mohd Noor F T, and Bakar A A 2007 Properties of ferrite-filled natural rubber composites *Polym. - Plast. Technol. Eng.* **46** (6) 641–650.
- [11] Ismail H, Shuhelmy S, and Edyham M R The effects of a silane coupling agent on curing characteristics and mechanical properties of bamboo fibre filled natural rubber composites *Eur. Polym. J.* **38** (1) 39–47.
- [12] Prema K H, Kurian P, Joy P A, and Anantharaman M R 2008 Physicomechanical and magnetic properties of neoprene based rubber ferrite composites *Polym. - Plast. Technol. Eng.* **47** (2) 137–146.
- [13] Khumpaitool B, Utara S, and Jantachum P 2018 Thermal and mechanical properties of an epoxidised natural rubber composite containing a Li/Cr co-doped NiO-based filler *J. Met. Mater. Miner.* **28** (1).